Transactions of the 17th International Conference on Structural Mechanics in Reactor Technology (SMiRT 17)
Prague, Czech Republic, August 17 –22, 2003
Paper # C03-5

Analysis of Power History Effect for Cladding Stress during Power Ramp by FEMAXI-IV

Shuhei Takeda[1)]

[1)] TEPCO Systems Corporation, Tokyo, Japan

ABSTRACT

This study was performed for the purpose of clarifying power history effects of cladding stress during power ramp using FEMAXI-IV code [1]. Analytical parameters of power histories are base power and burnup. In the cases of low burnup, the cladding stress is not influenced by the power history. However, in the cases of high burnup, the cladding stress is influenced by the base power. In these cases, the maximum cladding hoop stress during power ramp decreases with increase of base power. The most dominant parameter of this tendency is FP gas release model in the analytical code.

KEY WORDS: power history, cladding stress, power ramp, FEMAXI-IV, creep strain, MATPRO-Version 09 model, gap conductance, modified Ross & Stoute model, FP gas release, Turnbull model

INTRODUCTION

In the commercial BWR core operation, cladding stress due to Pellet Cladding Interaction (PCI) during Control Rod (CR) withdrawing is very important to prevent the failure of cladding. Since the cladding stress is much influenced by power history, it is very important to understand specific relation between the cladding stress and the power history. There are many fuel thermal mechanical analysis codes, for example FEMAXI, COMETHE [2], FRAPCON [3], INFRA [4], INTERPIN [5], STAV [6], TRANSURANUS [7] and so on. Though the many codes are closed codes, FEMAXI is open code—to utilize for fuel thermal mechanical analysis of the Light Water Reactor (LWR)—developed by Japan Atomic Energy Research Institute (JAERI). TEPSYS introduced FEMAXI-IV in 1997, and improved some models aiming at the elevation of prediction accuracy using Halden secret data, Interramp data [8], Superramp data [9] and Japanese commercial core irradiation secret data. Improved FEMAXI-IV has been used for the stress calculation to set the condition of CR withdrawing operation.

In this study, the cladding stress is calculated by FEMAXI-IV code as the parameter of the base power and burnup until the power ramp. Detailed evaluation was carried out paying attention to the 30 MWd/kgU burnup cases in which the influence of base power before power ramp appears.

CALCULATION CONDITIONS

Analyzed fuel is GE8 UO_2 and the main specifications of it are shown in Table 1. Calculation Code is FEMAXI-IV improved by TEPSYS (FEMAXI-T). Typical power history is shown in Fig. 1. The Linear Heat Generation Rate (LHGR) during the power ramp reaches to the maximum constant power depending on burnup—predicted to actually reach during CR withdrawing—after constant base power operation. Analytical parameters of the power history are constant base power and burnup before power ramp. These parameters are shown in Table 2 with other analytical conditions. Although the analytical condition such as constant low base power kept until high burnup is not realistic in commercial core operation, it was conditioned to clarify the base power effect for the cladding stress in this study. The power ramp rate is set 200 W/cm-min referred several power ramp tests. Compared with the pellet and the cladding thermal deformation, this power ramp rate is low enough, and the deformations of the pellet and the cladding could be regarded as steady state.

Table 1 Specifications of GE8 UO_2 fuel (called 8x8BJ in Japan)

Cladding outer diameter	1.23 cm
Cladding thickness	0.086 cm
Pellet outer diameter	1.03 cm
Plenum volume ratio	0.1
Initial helium pressure	0.3 MPa

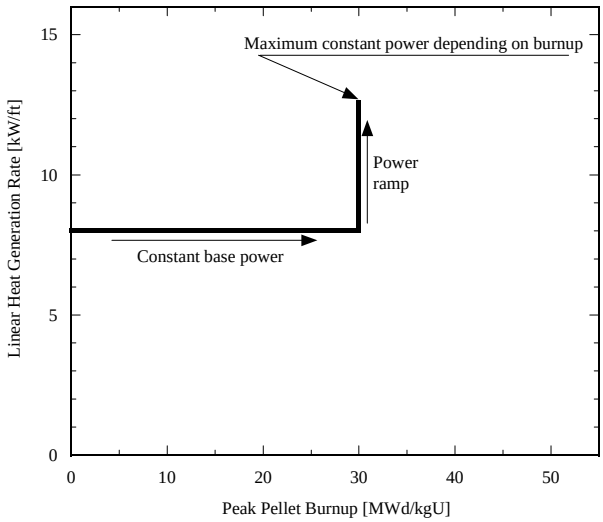

Fig.1 Typical Power history (Base Power = 8kW/ft , Burnup = 30MWd/kgU)

Table 2 Analytical conditions and parameters

Constant base power	2, 4, 6, 8, 10 kW/ft (1kW/ft = 32.8 W/cm)
Burnup at Power Ramp	10, 30, 50 MWd/kgU
Maximum power	Constant power depending on burnup
Power ramp speed	200 W/cm-min
Heat conduction	unsteady state calculation
Gas flow in gap	unsteady state calculation
Core pressure (Outer pressure)	7 MPa

CALCULATION RESULTS

Cladding stress during power ramp

The maximum hoop stresses of claddings during power ramp are shown in Fig. 2. In the cases of low burnup (e.g. 10 MWd/kgU), the influence of base power on the cladding stress has not clarified. However, in the cases of high burnup (e.g. 30 MWd/kgU), the tendency that the cladding stress is influenced by the base power appears. In these cases, the maximum cladding hoop stress during the power ramp decreases with increase of the base power. This result suggests that it is rational to operate with the higher base power for the high burnup fuel from the viewpoint of the structural integrity of the fuel rod. Therefore, the detailed evaluation—with interest in gap between the pellet and the cladding, temperature of the pellet and gap conductance—was carried out for the high burnup cases (30 MWd/kgU).

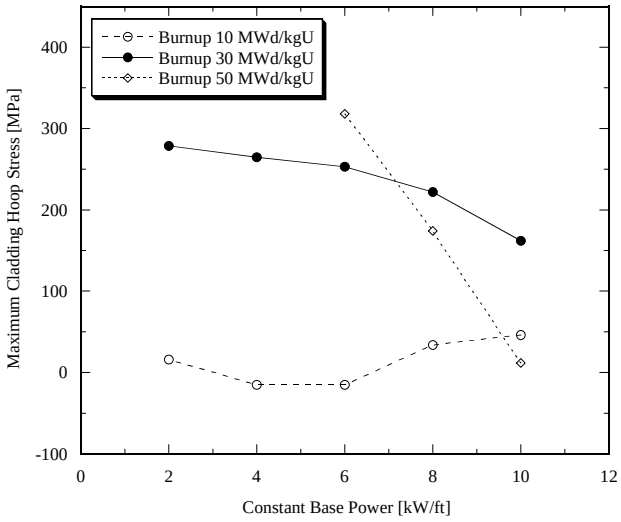

Fig.2 Maximum cladding hoop stress trend for base power and burnup

Gap before power ramp

Changes of the pellet and the cladding diameter in the base power and the power ramp conditions are shown in Fig. 3. Shrinkage of the cladding and swelling of the pellet increase with the base power. Consequently, the gap before the power ramp decreases with the

base power.

First, the relation between shrinkage of the cladding and the base power are considered. During nuclear reactor operation, the coolant pressure is putted as external pressure to the cladding. Since this external pressure is higher than the internal pressure due to discharge of FP gas and thermal expansion of the gas, the cladding is subjected to the external pressure during operation of the power plant. The creep strain rate of the cladding—MATPRO-Version 09 model [10] employed in FEMAXI-IV—is expressed with function of the cladding stress, temperature, and the fast neutron flux.

$$\dot{\varepsilon} = K\phi\left(\sigma + Be^{C\sigma}\right)\exp\left(-10{,}000/RT\right)t^{-\frac{1}{2}} \qquad (1)$$

Creep strain increases as the fast neutron flux, the cladding temperature, the stress and the irradiation time increase. If the base power increases, these 4 factors change such as below.

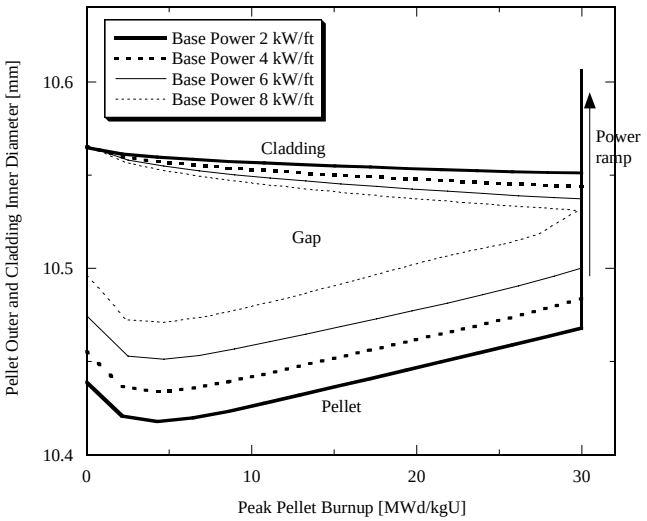

Fig.3 Changes of pellet outer and cladding inner diameter with burnup

* The fast neutron flux increases, because it is postulated that it is proportional to the LHGR in this calculation.
* The cladding temperature rises.
* The time shortens, because it is in inverse proportion to the LHGR.
* The stress decreases slightly, because the gap temperature rises, and the internal pressure increases and then the differential pressure decreases.

Table 3 Changes of cladding temperature with base power at 0 MWd/kgU burnup

Constant base power [kW/ft]	2	4	6	8	10
Cladding inner temperature [°C]	302	312	322	332	342
Cladding outer temperature [°C]	292	293	294	294	295

The fast neutron flux and the time effects are negated completely, because the creep strain is proportional to them in the model. Since the change of the stress has a small influence on creep strain, the difference of the cladding creep strain should be originated in the difference of the cladding temperature in the base power operation shown in Table 3. For these reasons, the shrinkage of the cladding increases with the base power.

Next, deformation of the pellet is considered. The amount of swelling of the pellet in FEMAXI-T depends only on the burnup of the fuel, therefore the difference of the pellet outer diameters in Fig. 3 are equal to the difference of the pellet temperature. Since the cladding stress during the power ramp is generated according to the difference of the diameter between the pellet and the cladding, the deformation of them will be evaluated in detail.

Change of diameter during power ramp

Changes of the pellet and the cladding diameter during power ramp are shown in Fig. 4. The open circle shows the point starting of the power ramp. The gap between the pellet and the cladding at the point starting of the power ramp is so large that the base power is low as shown in Fig. 3. A pellet expands due to heat-up with increase of LHGR, and the gap decreases gradually. Comparing the LHGR when the pellet contacts with the cladding for every base power cases, a smaller base power case has smaller LHGR. Moreover, when the diameters of the pellet in the same LHGR level are compared, it is larger in the case of lower base power. As mentioned above, the diameter of the pellet corresponds to the temperature of pellet. Hence, this result shows that the temperature of the lower base power case is higher than that of the higher base power case at the same LHGR during the power ramp. The pellet temperature during the power ramp is shown in Fig. 5. The tendency that the temperature of the pellet in the lower base power case is higher than that of the higher base power case. The temperature of the pellet is totally dependent on the heat transfer at the cladding outer surface, the thermal conductivity of the cladding and the pellet, and the gap conductance between the pellet and the cladding. The heat transfer coefficient at the cladding outer surface and the thermal conductivity of the cladding and the pellet—although, they have temperature dependence—are not greatly different in each case. Therefore, the parameter, which should be paid attention, is the gap conductance.

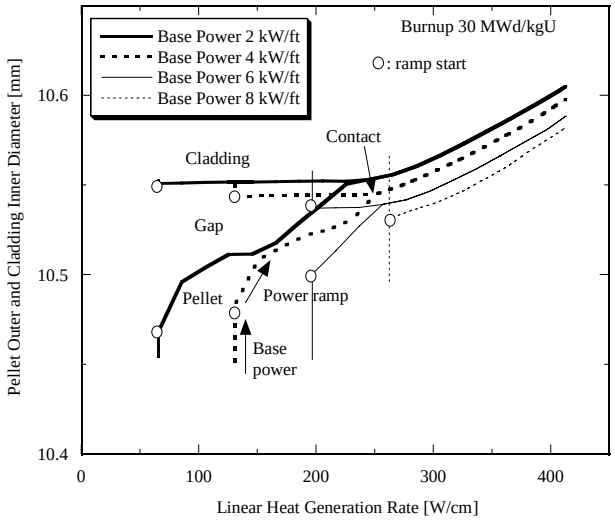

Fig.4 Changes of pellet outer and cladding inner diameter with LHGR

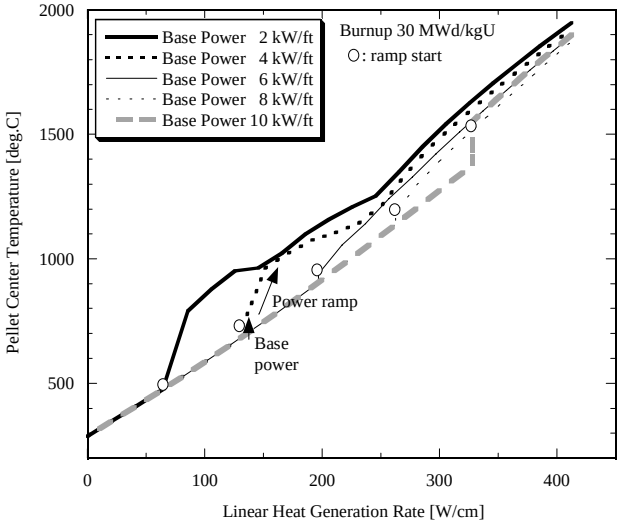

Fig.5 Changes of pellet center temperature with LHGR

Gap conductance in power ramp

The gap conductance is expressed by modified Ross and Stoute model [11]. A gap conductance is mainly dependent on the gap width between the cladding and the pellet, the physical properties of the gas in the gap, contact pressure in the model. When the thermal conductivity of the gas in the gap is low, the gap conductance is low even if the gap is narrow. As shown in Fig. 4 and Fig. 5, since the pellet temperature differs in each analytical case after the pellet contacts the cladding, it is thought that this difference comes from the difference of thermal conductivity of the gas in the gap. In early stages, although the cladding is filled up with helium gas, the thermal conductivity of FP gas (e.g. zenon or krypton) which are released from the pellet are 1 or more orders lower than helium gas. From this, it is guessed easily that the difference of the thermal conductivity of the gas in the gap is influenced by the amount of FP gas. The relation between the gap width and the gap conductance are shown in Fig. 6 and Fig. 7. A gap conductance in the lower base power case is lower compared to the high base power case with regardless of the gap width. Consequently, in these two cases, the amounts of released FP gas to the gap differ clearly.

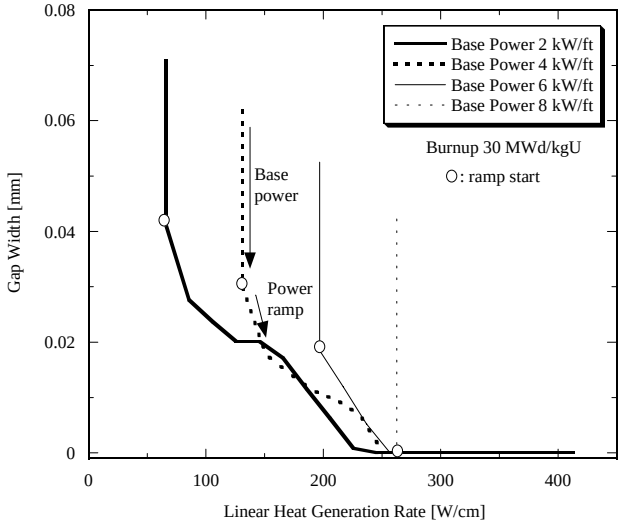

Fig.6 Changes of gap width with LHGR

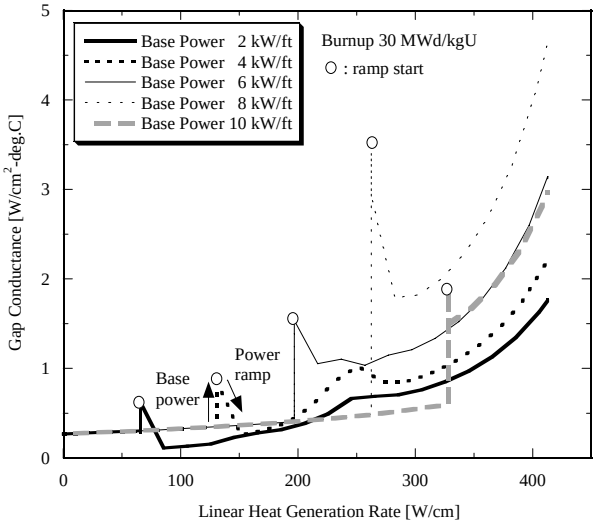

Fig.7 Changes of gap conductance with LHGR

The amount of released FP gas to the gap is mainly decided by the quantity of FP accumulated in inter-granular during the base power operation. FP gas generated within a grain is diffused in inter-granular, and the diffusion coefficient is expressed by Turnbull Model [12]—with a function of temperature—shown in Fig. 8. If base power is lower than 6 kW/ft, the center temperature of the pellet is less than 1200 K, and FP gas diffusion rate is constant. Therefore, in the cases of the same burnup, many FP gas will be accumulated in the inter-granular in the case of lower base power cases, because of long combustion time. Since a diffusion coefficient becomes extremely large when the base power exceeds this level, the amount of FP gas diffused to inter-granular increases in the case of high base power. FP gas accumulated in the inter-granular is released to the gap during the power ramp when the amount of diffused FP gas exceeding saturation limit expressed with the following formulas.

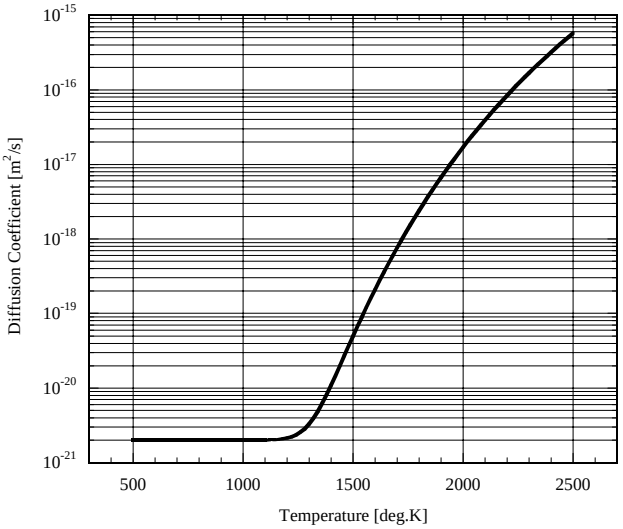

Fig.8 FP gas diffusion coefficient trend for temperature (Turnbull model)

$$N_f^{max} = \frac{4 r_f f_f(\vartheta)}{3kT \sin^2 \vartheta} f_b \left(\frac{2\gamma}{r_r} + P_{ext} \right) \quad (2)$$

Here, amount of released FP gas to the gap before and after the power ramp is as shown in Fig. 9. The amount of FP gas released to the gap is decreases gradually with increase of the base power from 2 to 6kW/ft. As this result, the gap conductance decreases in the case of low base power. In the case of 8kW/ft, although more amounts of FP gas released than the case of 6kW/ft, the gap conductance is also larger than the case of 6kW/ft, and this result does not agree with other tendencies. The reason is expected that this inconsistency arises from the deference of the calculation models employed in heat and stress calculation in FEMAXI-T. The pellet and cladding contact pressure calculated in heat analysis—the simplified model is used in it—is larger than that of specific stress analysis. This problem should be improved in the future works.

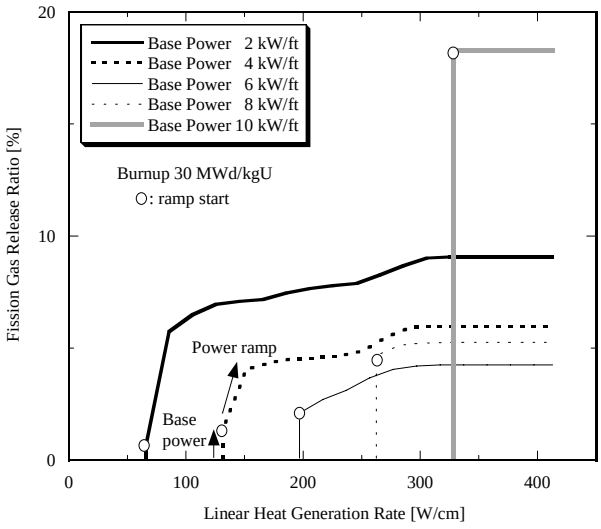

Fig.9 Changes of fission gas release with LHGR

Another cases which the gap has already closed

At 30 MWd/kgU of the high base power cases about over 8 kW/ft, the gap has already closed and the cladding has been deformed to the outside by the PCI creep before power ramp. Since the maximum LHGR during the power ramp are same, the increment of LHGR during the power ramp decreases with increase of the base power. This is the most dominant effect in these cases and the cladding deformation during power ramp decreases with the base power. Therefore, the maximum cladding stress decreases with the base power even if the cases which the gap has already closed before the power ramp.

There are not enough data to confirm this tendency. Therefore, the useful experimental data should be researched and the FP gas release model and its sensitivity for the cladding stress should be verified using them as a future work.

CONCLUSION

In the commercial BWR core operation, cladding stress during CR withdrawing is very important factor for the cladding failure by PCI. Since the cladding stress is much influenced by power history, it is very important to grasp the power history effect on the cladding stress.

The maximum cladding stress during power ramp decreases with increase of base power. Because the FP gas release increases with decrease of the base power and has much effect on the cladding stress during power ramp than the effect of the cladding shrinkage by core pressure creep. This result suggests that it is more advantageous to operate with the higher base power for the high burnup fuel from the viewpoint of the structural integrity of the fuel rod. However, there are not enough data to confirm this tendency. Therefore, the useful experimental data should be researched and the FP gas release model and its sensitivity for the cladding stress should be verified using them as a future work.

NOMENCLATURE

$\dot{\varepsilon}$ - 2 axial creep strain velocity, m/m-sec
K - 5.129×10^{-29}
B - 7.252×10^{2}
C - 4.967×10^{-8}
R - 1.987, cal/mol-K
T - Temperature, K
t - Time, sec
ϕ - Fast neutron flux, n/m^2-sec (E>1.0 MeV)
σ - Hoop stress, N/m^2
N_f^{max} - Amount of saturation of FP gas atoms per unit square in intergranular area, atoms/cm^2
r_f - Radius of gas bubbles in intergranular area, cm
$f_f(\vartheta)$ - A Lens-like bubble volume ratio per a sphere
ϑ - Angle of lens-like bubble, degrees
k - Number of Boltzmann (= 1.38×10^{-16}), erg/k
γ - Surface tension (= 626), erg/cm^2
f_b - Ratio of lens-like bubbles area per intergranular area
P_{ext} - External pressure, dyne/cm^2

REFERENCES

1. Motue SUZUMI and Hiroaki SAITOU, Description and User's Manual of the Light Water Reactor Fuel Analysis Code FEMAXI-IV (Ver.2), JAERI-Data/Code 97-010, Feb 1997.
2. J. van Vliet and M. Billaux, Comparison with Experiment of COMETHE III-L Fuel Rod Behaviour Predictions, K19830586 (0-85334-217-2) Water React Fuel Elem Perform Comput Model Page 605-619,1983.
3. Lanning D D, Beyer C E and Geelhood K J, Comparison of the NRC Fuel Performance code FRAPCON-3 to Independent Data Sources, E0387B (TANSA) (0003-018X) Trans Am Nucl Soc Vol.77 Page 69-71, 1997.
4. Lee C B, Yang Y S, Bang J G, Kim D H, Kim Y M, Jung Y H, UO2 Fuel Rod Performance Analysis Code, INFRA Development, JAERI-CONF-2002-009 Page 438-458, 2002.
5. Kjaer-Pedersen N, INTERPIN LAB: Automating Fuel Performance Analysis Using MS-Access, E0387B (TANSA) (0003-018X) Trans Am Nucl Soc Vol. 81 Page 76-78 1999, 1999
6. Ali Massih and Zbigniew Weiss, STAV7.0 Model Description, BU 97-091, Sep 1997.
7. Lassmann K, TRANSURANUS: a fuel rod analysis code ready for use in simulators and plant analyzers, K19950066 (951-38-4092-1) CSNI Spec Meet Simul Plant Anal, Page 185-204, 1994.
8. H. Mogard et al, The Studsvik Inter-Ramp Project : An International Power Ramp Experimental Program, ANS (1979)
9. H. Mogard et al, The International Super Ramp Project at Studsvik, ANS (1985)
10. MATPRO-09, A Handbook of Materials Properties for Use in the Analysis of Light Water Reactor Fuel Rod Behavior, USNRC TREE NUREG-1005 (1976)
11. Ross A.M. and Stoute R.L., Heat Transfer Coefficient between UO_2 and Zircaloy-2, CRFD-1075 (1962)
12. Turnbull J.A., Friskney C.A., et al., The Diffusion Coeffcients of Gaseous and Volatile Species during the Irradiation of Uranium Dioxide, J. Nucl. Mater., 107(1982)168-184.